Journal of the Earth and Space Physics, Vol. 44, No. 4, Winter 2019, P. 29-39
DOI: 10.22059/jesphys.2018.247879.1006954

Large-scale Inversion of Magnetic Data Using Golub-Kahan Bidiagonalization with Truncated Generalized Cross Validation for Regularization Parameter Estimation

Vatankhah, S.*

Assistant Professor, Department of Earth Physics, Institute of Geophysics, University of Tehran, Iran

(Received: 20 Dec 2017, Accepted: 15 May 2018)

Abstract
In this paper a fast method for large-scale sparse inversion of magnetic data is considered. The L_1-norm stabilizer is used to generate models with sharp and distinct interfaces. To deal with the non-linearity introduced by the L_1-norm, a model-space iteratively reweighted least squares algorithm is used. The original model matrix is factorized using the Golub-Kahan bidiagonalization that projects the problem onto a Krylov subspace with a significantly reduced dimension. The model matrix of the projected system inherits the ill-conditioning of the original matrix, but the spectrum of the projected system accurately captures only a portion of the full spectrum. Equipped with the singular value decomposition of the projected system matrix, the solution of the projected problem is expressed using a filtered singular value expansion. This expansion depends on a regularization parameter which is determined using the method of Generalized Cross Validation (GCV), but here it is used for the truncated spectrum. This new technique, Truncated GCV (TGCV), is more effective compared with the standard GCV method. Numerical results using a synthetic example and real data demonstrate the efficiency of the presented algorithm.

Keywords: Magnetic survey, Sparse inversion, Golub-Kahan bidiagonalization, Regularization parameter estimation, Truncated generalized cross validation.

1. Introduction
The inversion of magnetic field data encloses many practical difficulties. Most importantly, the solution of the problem is not unique. While the physics of the problem introduces inherent ambiguity in the solution, algebraic ambiguity arises because the number of measurements is considerably smaller than the number of unknown model parameters in the discretized subsurface (Li and Oldenburg, 1996; Pilkington, 1997). The determination of the solution becomes further complicated by the contamination of the observations by noise, which is amplified in the inversion process due to the ill-conditioning of the model matrix. Therefore, in order to estimate a stable and geologically meaningful solution, it is necessary to both impose additional constraints on the model and apply regularization (Portniaguine and Zhdanov, 1999). Finally, seeking a three-dimensional model of the subsurface presents a computational challenge, and powerful algorithms are needed to reduce both memory and CPU requirements of the computing systems (Li and Oldenburg, 2003; Pilkington, 2009; Portniaguine and Zhdanov, 2002; Boulanger and Chouteau, 2001). This paper addresses these issues through the use of an appropriately constrained edge-preserving regularization, implemented through a computationally efficient iterative algorithm for finding the solution in a relevant subspace, and extends the introduced approach for the solution of the gravity inverse problem presented in Vatankhah et al. (2017).

For the inversion of magnetic data, standard methods proceed with the minimization of a global objective function comprising a data misfit and stabilizing regularization terms. For data misfit term, a weighted L_2-norm error between the observed and predicted data due to the inverse solution is typically used (Li and Oldenburg, 1996; Pilkington, 2009; Portniaguine and Zhdanov, 1999). Depending on the type of desired model features to be recovered through the inversion, there are several choices for the stabilizer. The general inversion methodology developed by Li and Oldenburg (1996) employs stabilization by L_2-norm regularization with respect to the low-order finite difference approximation of the derivatives of the model parameters in each of the three orthogonal directions. The approach has been successfully applied in a

*Corresponding author: svatan@ut.ac.ir

wide range of the geophysical applications but yields relatively smooth models that are not always consistent with real geological structure (Farquharson, 2008). On the other hand, stabilization with a Minimum Support (MS) or Minimum Gradient Support (MGS) function yields models that provide better contrast (Last and Kubic, 1983; Portniaguine and Zhdanov, 1999; Vatankhah et al., 2014, 2015). Sharp and focused images of the subsurface can also be achieved using the L_1-norm stabilizer (Loke et al., 2003; Farquharson, 2008; Vatankhah et al., 2017) and with the sparseness constraint introduced by the use of the Cauchy norm applied to the model parameters (Pilkington, 2009). Recently, a method for adaptively recovering both smooth and blocky models was developed by Sun and Li (2014). The current study uses the L_1-norm stabilization, which is implemented by an Iteratively Reweighted Least Squares (IRLS) algorithm and was studied for gravity data inversion in Vatankhah et al. (2017).

To provide an algorithm that is effective for large problems, it is important to use a computationally efficient approach. The methodology in Pilkington (2009) adopts a conjugate gradient algorithm for efficient solution of the underlying large-scale systems of equations, that is adopted in Li and Oldenburg (2003) and Pilkington (1997), as well. An alternative is to use the Golub-Kahan bidiagonalization (sometimes called Lanczos bidiagonalization) of the model matrix, which leads to a hybrid LSQR algorithm (Chung et al., 2008; Kilmer and O'Leary, 2001). An extensive discussion of the multiplicity of the techniques for finding the regularization parameter in the objective function, which provides the trade-off between the data misfit and the stabilizing terms, is provided in Vatankhah et al. (2017) and references therein. The method developed here is based on an extension of the Generalized Cross Validation (GCV) rule for using with the hybrid LSQR algorithm. This further expands the approach presented in Vatankhah et al. (2017), which adopted a truncation for the Unbiased Predictive Risk Estimator (UPRE), but at the same time, requires knowledge of the underlying noise distribution in the measured data that is not needed for the GCV related techniques.

The rest of the current paper is organized as follows. In section 2, the inversion methodology is described based on the L_1-norm stabilizer. The solution of the inverse problem using the hybrid LSQR algorithm and methods for estimating the regularization parameter with respect to the Krylov subspace are discussed in sections 2.1 and 2.2, respectively. Furthermore, the application of the SVD at the subspace level for both the inverse solution and parameter-choice method is shown in section 2.2. In section 3, the results of the presented algorithm applied on a synthetic model consisting of multiple bodies are demonstrated. The aeromagnetic data over a portion of the Wuskwatim Lake, Manitoba, Canada is inverted and the results are presented in section 4. The Conclusion is also given in section 5.

2. Inversion methodology

The subsurface volume is divided into a large number of cubes of fixed size but unknown susceptibility. This allows maximum flexibility for the model to represent the subsurface structures (Li and Oldenburg, 1996; Boulanger and Chouteau, 2001; Liu et al., 2015). For the inversion methodology presented here, it is assumed that there is no remanent magnetization and only the induced magnetization is considered. This magnetization is uniform within each cube and is given by the product of the susceptibility (κ) and the induced geomagnetic field (Li and Oldenburg, 1996). The susceptibilities of the cubes are collected in a vector $\boldsymbol{m} = (\kappa_1, \kappa_2, ..., \kappa_n)^T$ where n is the total number of the cubes, and $\boldsymbol{d}^{obs} \in \mathbb{R}^m$ contains the measured total magnetic field data. The relationship between the observed data and model parameters is given by:

$$\boldsymbol{d}^{obs} = G\boldsymbol{m} \tag{1}$$

In Equation (1), the sensitivity matrix $G \in \mathbb{R}^{m \times n}$, $m \ll n$, has elements g_{ij} that represent the effect of unit susceptibility in the j^{th} cell calculated on the i^{th} data location. A simplified and computationally fast formula for evaluating the total field of a cube analytically was developed by Rao and Babu (1991), and is used here to form the

elements of the sensitivity matrix. Thus, given G and $\boldsymbol{d}^{obs}$, the goal of the inversion is to find a stable and geologically meaningful susceptibility model that reproduces the observed data at the noise level.

As mentioned in previous section, problem (1) is ill-posed and an acceptable solution may be found from the minimization of the following objective function (Vatankhah et al., 2017):

$$\Phi(\boldsymbol{m},\alpha)=\left\|W_d\left(G\boldsymbol{m}-\boldsymbol{d}^{obs}\right)\right\|_2^2+\alpha^2\left\|\boldsymbol{m}-\boldsymbol{m}_{apr}\right\|_1\approx\left\|W_d\left(G\boldsymbol{m}-\boldsymbol{d}^{obs}\right)\right\|_2^2+\alpha^2\left\|W_{L1}\left(\boldsymbol{m}-\boldsymbol{m}_{apr}\right)\right\|_2^2 \quad (2)$$

Here, the L_1-norm stabilizer is approximated with a L_2-norm term via introducing $W_{L1}=diag\left(\left(\left(\boldsymbol{m}-\boldsymbol{m}_{apr}\right)^2+\varepsilon^2\right)^{-1/4}\right)$ for a very small $\varepsilon^2\approx10^{-9}$ (Wohlberg and Rodriguez, 2007; Voronin, 2012; Vatankhah et al., 2017). The vector $\boldsymbol{m}_{apr}$ contains known reference information on the parameters, perhaps estimated from prior geological or geophysical investigation or it can be set to $\mathbf{0}$ (Li and Oldenburg, 1996). Weighting matrix W_d is square and diagonal with elements $1/\sigma_i, i=1:m$, where σ_i is the standard deviation of the noise in the i^{th} datum assuming that the noise in $\boldsymbol{d}^{obs}$ is uncorrelated and Gaussian. Following Farquharson and Oldenburg (2004), it is assumed that the absolute magnitudes of the errors are unknown, but the relative magnitudes can be estimated. The matrix W_{L1} depends on the model parameters and then the problem is non-linear and the sparse model that solves (2) is approximated by iteratively finding the solutions $\boldsymbol{m}^{(k)}$ of the Tikhonov functions:

$$\Phi^{(k)}\left(\boldsymbol{m}^{(k)},\alpha^{(k)}\right)=\left\|W_d\left(G\boldsymbol{m}^{(k)}-\boldsymbol{d}^{obs}\right)\right\|_2^2+\left(\alpha^{(k)}\right)^2\left\|W_{L1}^{(k)}\left(\boldsymbol{m}^{(k)}-\boldsymbol{m}^{(k-1)}\right)\right\|_2^2 \quad (3)$$

for $k=1,...,$ an initial model $\boldsymbol{m}^{(0)}=\boldsymbol{m}_{apr}$, and $W_{L1}^{(1)}=I_n$. Model weighting matrix is updated as $W_{L1}^{(k)}=diag\left(\left(\left(\boldsymbol{m}^{(k-1)}-\boldsymbol{m}^{(k-2)}\right)^2+\varepsilon^2\right)^{-1/4}\right)$ for $k>1$. It worth noting that in Equation (3), the regularization parameter α which balances the two terms is explicitly dependent on the iteration number k. Furthermore, to compensate for the natural decay of the kernel, the diagonal depth weighting matrix, $W_{depth}=1/z_j^{\beta}$, is introduced in Equation (3), replacing $W_{L1}^{(k)}$ by $W^{(k)}=W_{L1}^{(k)}W_{depth}$ (Li and Oldenburg, 1996; Boulanger & Chouteau, 2001). Here, z_j is the mean depth of the cell j and β is a weighting parameter. Theoretically, $\boldsymbol{m}^{(k)}$ is obtained by minimizing Equation (3), as explained in Vatankhah et al. (2017), which leads to the expression:

$$\boldsymbol{m}^{(k)}=\boldsymbol{m}^{(k-1)}+\left(W^{(k)}\right)^{-1}\left(\tilde{\tilde{G}}^T\tilde{\tilde{G}}+\left(\alpha^{(k)}\right)^2I_n\right)^{-1}\tilde{\tilde{G}}^T\tilde{\boldsymbol{r}}^{(k)}=\boldsymbol{m}^{(k-1)}+\left(W^{(k)}\right)^{-1}\boldsymbol{h}^{(k)} \quad (4)$$

Here, matrix $\tilde{\tilde{G}}=W_dG\left(W^{(k)}\right)^{-1}$, $\tilde{\boldsymbol{r}}^{(k)}=W_d\left(\boldsymbol{d}^{obs}-G\boldsymbol{m}^{(k-1)}\right)$ and update $\boldsymbol{h}^{(k)}$ solves the regularization problem:

$$\Phi^{(k)}\left(\boldsymbol{h}^{(k)},\alpha^{(k)}\right)=\left\|\tilde{\tilde{G}}\boldsymbol{h}^{(k)}-\tilde{\boldsymbol{r}}^{(k)}\right\|_2^2+\left(\alpha^{(k)}\right)^2\left\|\boldsymbol{h}^{(k)}\right\|_2^2 \quad (5)$$

Practically, susceptibility limits $\kappa_{\min}$ and $\kappa_{\max}$ should be used at each iteration to reduce the non-uniqueness of the problem by projecting values of the $\boldsymbol{m}^{(k)}$ that lie outside $[\kappa_{\min},\kappa_{\max}]$ to the nearest limit. The iteration terminates when either the solution satisfies the threshold error level, or a predefined maximum number of iterations ($K_{\max}$) is reached (Li and Oldenburg, 1996; Boulanger & Chouteau, 2001).

2-1. The LSQR algorithm

The LSQR algorithm is used to find the solution of Equation (5) at each iteration (Paige and Saunders, 1982a, b), in which the Golub-Kahan Bidiagonalization (GKB)

process is used for projection of the problem to a krylov subspace of much smaller dimension. Given a matrix $\tilde{\tilde{G}}$ and a vector $\tilde{\boldsymbol{r}}$, t steps of GKB process compute the decomposition:

$$\tilde{\tilde{G}}A_t = H_{t+1}B_t, \qquad H_{t+1}\boldsymbol{e}_{t+1} = \tilde{\boldsymbol{r}}/\|\tilde{\boldsymbol{r}}\|_2 \tag{6}$$

Here, Matrix $B_t \in \mathbb{R}^{(t+1)\times t}$ is bidiagonal, $\boldsymbol{e}_{t+1}$ is the unit vector of length $t+1$, and matrices $H_{t+1} \in \mathbb{R}^{m\times(t+1)}$ and $A_t \in \mathbb{R}^{n\times t}$ are column orthogonal, (Hansen, 2007). The Columns of A_t span a Krylov subspace in which an approximate solution $\boldsymbol{h}_t$ that lies in this subspace will have the form $\boldsymbol{h}_t = A_t\boldsymbol{z}_t$, where $\boldsymbol{z}_t$ is a vector of length t. The column orthogonality of matrix H_{t+1} leads to replacement of data misfit term $\left\|\tilde{\tilde{G}}\boldsymbol{h} - \tilde{\boldsymbol{r}}\right\|_2^2$ in Equation (5) by a data misfit related to the projected solution:

$$\left\|B_t\boldsymbol{z}_t - \boldsymbol{c}\right\|_2^2 \tag{7}$$

where $\boldsymbol{c} = \|\tilde{\boldsymbol{r}}\|_2\,\boldsymbol{e}_{t+1}$ (Kilmer and O'Leary, 2001; Chung et al., 2008; Gazzola and Nagy, 2014). Furthermore, by the column orthogonality of A_t, $\|\boldsymbol{h}_t\|_2^2 = \|\boldsymbol{z}_t\|_2^2$. Equation (5) is then replaced by the regularized projected problem (Vatankhah et al., 2017):

$$\Phi^{(k)}\left(\boldsymbol{z}_t, \alpha^{(k)}\right) = \left\|B_t\boldsymbol{z}_t - \boldsymbol{c}\right\|_2^2 + \left(\alpha^{(k)}\right)^2\left\|\boldsymbol{z}_t\right\|_2^2 \tag{8}$$

Under the assumption that $t \ll \min(m,n)$, finding the solution of Equation (8) is more efficient than solving Equation (5), and therefore we can replace Equation (4) by:

$$\boldsymbol{m}_t^{(k)} = \boldsymbol{m}_t^{(k-1)} + \left(W^{(k)}\right)^{-1}A_t^{(k)}\boldsymbol{z}_t^{(k)} \tag{9}$$

for a projected problem of size t at iteration k. Note that both $\tilde{\tilde{G}}$ and $\tilde{\boldsymbol{r}}$, and then the factorization of Equation (6) depends on k.

It is clear that for a given k, the projected solution $\boldsymbol{z}_t(\alpha)$ depends on both subspace size t and regularization parameter α. As described in Vatankhah et al. (2017), the focus here is the estimation of an optimal α for a given t and k. More details on finding an optimum t can be found in Renaut et al. (2017). The method described here allows the user to choose small t values and hence it is very effective in reducing the computational time.

2-2. Regularization parameter estimation

Whether solving Equation (5), or Equation (8) for a fixed t, an approach for determining the regularization parameter $\alpha^{(k)}$ is required. Amongst many possibilities, the GCV method has received significant attention in conjunction with the solution of the projected problem (Kilmer and O'Leary, 2001; Chung et al., 2008; Renaut et al., 2017). GCV is a statistical technique that is independent from knowing prior information about the noise in data; rather it seeks extracting such information from the observations. It is based on the leave one out principle in which if a measurement is removed from the data set, the corresponding regularized solution should provide a good estimate for the removed measurement (Golub et al., 1979). The GCV function to be minimized is given by (Renaut et al., 2017):

$$G(\alpha,t) = \frac{\left\|\left(B_tB_t(\alpha) - I_{t+1}\right)\boldsymbol{c}\right\|_2^2}{\left(trace\left(I_{t+1} - B_tB_t(\alpha)\right)\right)^2} \tag{10}$$

where, $B_t(\alpha) = \left(B_t^TB_t + \alpha^2I_t\right)^{-1}B_t^T$. However, it has been demonstrated that using $\alpha_{opt} = \arg\min\left\{G(\alpha,t)\right\}$ for the projected problem may lead to solutions which are over-smoothed (Chung et al., 2008). Here, I will further examine the GCV for solving Equation (8) and introduce a truncated version of the method, denoted by Truncated GCV, which is more effective. This method is motivated by recent results of the truncated version of the UPRE parameter-choice rule applied on projected gravity inverse problems (Vatankhah et al., 2017).

To obtain the TGCV, I use the singular value decomposition of B_t given by $B_t = \sum_{i=1}^{t}\gamma_i\boldsymbol{u}_i\boldsymbol{v}_i^T$, (Golub and Van Loan, 1996), where the singular values are ordered as $\gamma_1 \geq \gamma_2 \geq \ldots \geq \gamma_t > 0$ and $\boldsymbol{u}_i$ and $\boldsymbol{v}_i$ are the columns of the orthonormal matrices

$U \in \mathbb{R}^{(t+1)\times(t+1)}$ and $V \in \mathbb{R}^{t\times t}$, respectively. Introducing the filter factors $f_i(\alpha) = \gamma_i^2 \big/ \left(\alpha^2 + \gamma_i^2\right)$, the solution of Equation (8) and the GCV are given by (Renaut et al., 2017):

$$\boldsymbol{z}_t(\alpha) = \sum_{i=1}^{t} f_i(\alpha) \frac{\boldsymbol{u}_i^T \boldsymbol{c}}{\gamma_i} \boldsymbol{v}_i \tag{11}$$

$$G(\alpha, t) = \frac{\sum_{i=1}^{t} \left(1 - f_i(\alpha)\right)^2 \left(\boldsymbol{u}_i^T \boldsymbol{c}\right)^2 + \sum_{i=t+1}^{t+1} \left(\boldsymbol{u}_i^T \boldsymbol{c}\right)^2}{\left(1 + t - \sum_{i=1}^{t} f_i(\alpha)\right)^2} \tag{12}$$

Replacing B_t in Equation (10) by the best approximation of rank t', for $t' < t$, yields TGCV by replacing t in (12) by t'. Given α as the optimum value for the TGCV, the solution is reconstructed using (11), specifically with t and not t'. Thus, the TGCV method does not correspond to taking the filtered TSVD solution. Instead, α is chosen to appropriately regularize the first t' terms, whereas choosing α to regularize t terms will lead to a larger α to handle the additional terms, so that the dominant terms are then over smoothed. In the following, it is shown that the method of the TGCV leads to the solutions with less error as compared with the GCV. For the inversion algorithm presented here, $0.7t \le t' \le t$ is used based on heuristic presented in Vatankhah et al. (2017) for Truncated UPRE parameter-choice method. The steps are summarized in Table 1, which demonstrates the procedure to find the estimated models from inverting the magnetic data.

Table 1. Iterative inversion of magnetic data using GKB with TGCV parameter-choice rule

Inputs: $\boldsymbol{d}^{obs}$, $\boldsymbol{m}_{apr}$, G, W_d, $\varepsilon > 0$, $\kappa_{\min}$, $\kappa_{\max}$, t, $K_{\max}$.

1: Calculate W_{depth}, $\tilde{G} = W_d G$, and $\tilde{\boldsymbol{d}}^{obs} = W_d \boldsymbol{d}^{obs}$

2: Initialize $\boldsymbol{m}^{(0)} = \boldsymbol{m}_{apr}$, $W_{L1}^{(1)} = I_n$, $W^{(1)} = W_{depth}$

3: Calculate $\tilde{\boldsymbol{r}}^{(1)} = \tilde{\boldsymbol{d}}^{obs} - \tilde{G}\boldsymbol{m}^{(0)}$, $\tilde{\tilde{G}}^{(1)} = \tilde{G}\left(W^{(1)}\right)^{-1}$, $\tilde{\boldsymbol{r}}^{(1)} = \tilde{\boldsymbol{d}}^{obs} - \tilde{G}\boldsymbol{m}^{(0)}$, $k = 0$

4: **While** not converged, noise level not satisfied, or $k < K_{\max}$ **do**

5: $k = k + 1$

6: Apply GKB: $\tilde{\tilde{G}}^{(k)} A_t^{(k)} = H_{t+1}^{(k)} B_t^{(k)}$, $H_{t+1}^{(k)} \boldsymbol{e}_{t+1} = \tilde{\boldsymbol{r}}^{(k)} \big/ \left\|\tilde{\boldsymbol{r}}^{(k)}\right\|_2$

7: Find SVD: $B_t^{(k)} = U \Gamma V^T$. Calculate $\boldsymbol{c} = \left\|\tilde{\boldsymbol{r}}\right\|_2 \boldsymbol{e}_{t+1}$

8: For $k > 1$ estimate $\alpha^{(k)}$ using TGCV (or GCV)

9: Set $\boldsymbol{z}_t^{(k)} = \sum_{i=1}^{t} \frac{\gamma_i^2}{\left(\alpha^{(k)}\right)^2 + \gamma_i^2} \frac{\boldsymbol{u}_i^T \boldsymbol{c}}{\gamma_i} \boldsymbol{v}_i$

10: Set $\boldsymbol{m}_t^{(k)} = \boldsymbol{m}_t^{(k-1)} + \left(W^{(k)}\right)^{-1} A_t^{(k)} \boldsymbol{z}_t^{(k)}$

11: Impose constraint conditions on $\boldsymbol{m}_t^{(k)}$ to force $\kappa_{\min} \le \boldsymbol{m}_t^{(k)} \le \kappa_{\max}$

12: Calculate residual $\tilde{\boldsymbol{r}}^{(k+1)} = \tilde{\boldsymbol{d}}^{obs} - \tilde{G}\boldsymbol{m}^{(k)}$

13: Set $W_{L1}^{(k+1)} = diag\left(\left(\left(\boldsymbol{m}^{(k)} - \boldsymbol{m}^{(k-1)}\right)^2 + \varepsilon^2\right)^{-1/4}\right)$ and $W^{(k+1)} = W_{L1}^{(k+1)} W_{depth}$

14: Calculate $\tilde{\tilde{G}}^{(k+1)} = \tilde{G}\left(W^{(k+1)}\right)^{-1}$

15: **End while**

Outputs: Solution $\kappa = \boldsymbol{m}^{(k)}$ and $K = k$.

3. Synthetic example

In this section, the inversion methodology presented in Table 1 is validated using a model consisting of six different bodies. The dimensions and susceptibility of each body are given in Table 2. Figure 1a shows a perspective view of the model. Furthermore, four plan-sections of the model are shown in Figure 2. The surface magnetic data, $\boldsymbol{d}^{exact}$, are generated on a 100×50 grid with 20 m spacing. The intensity of the geomagnetic field is 47000 nT, and inclination and declination are I=50° and D=2°, respectively. The zero mean Gaussian random noise with standard deviation of $\left(0.02\left(\boldsymbol{d}^{exact}\right)_i + 0.002\left\|\boldsymbol{d}^{exact}\right\|_2\right)$ is added to each datum. Figure 1b shows the noise contaminated data. The subsurface is divided into 100×50×15=75000 cubes of dimension 20 m. The inversion is implemented via $\boldsymbol{m}_{apr} = \boldsymbol{0}$, $[\kappa_{\min} = 0, \kappa_{\max} = 0.06]$ and $K_{\max} = 50$. I emphasize that t in Algorithm 1 should be selected as small as possible ($t \ll \min(m,n)$) in order to provide an efficient algorithm, while it simultaneously captures the condition of the original kernel. Based on a previous investigation by Vatankhah et al. (2017), a value of $t \geq m/20$ is suitable for subspace dimension. Therefore, $t = 300$ is selected; yielding a matrix B_t of size 301×300. The test is performed on a desktop computer, Intel Core i7-4790 CPU 3.6 GH.

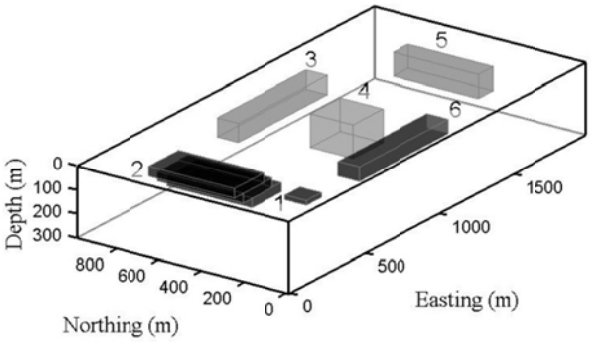

(a)

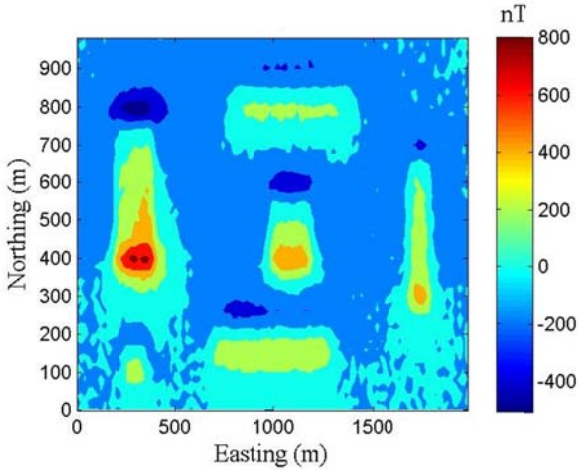

(b)

Figure 1. (a) A synthetic Model comprising six different bodies. Dark and grey bodies have the susceptibilities 0.06 and 0.04, respectively; (b) The noise contaminated magnetic anomaly associated with the model. Intensity of the geomagnetic field, inclination, and declination are 47000 nT, 50°, and 2°, respectively.

Table 2. The susceptibility and dimensions of each body for the model displayed in Figure 1.

Source number	Dimensions (m)	Depth to the surface (m)	Susceptibility (SI)
1	100×100×20	20	0.06
2	200×400×120	20	0.06
3	600×100×80	40	0.04
4	200×200×140	20	0.04
5	100×400×100	20	0.04
6	600×100×60	40	0.06

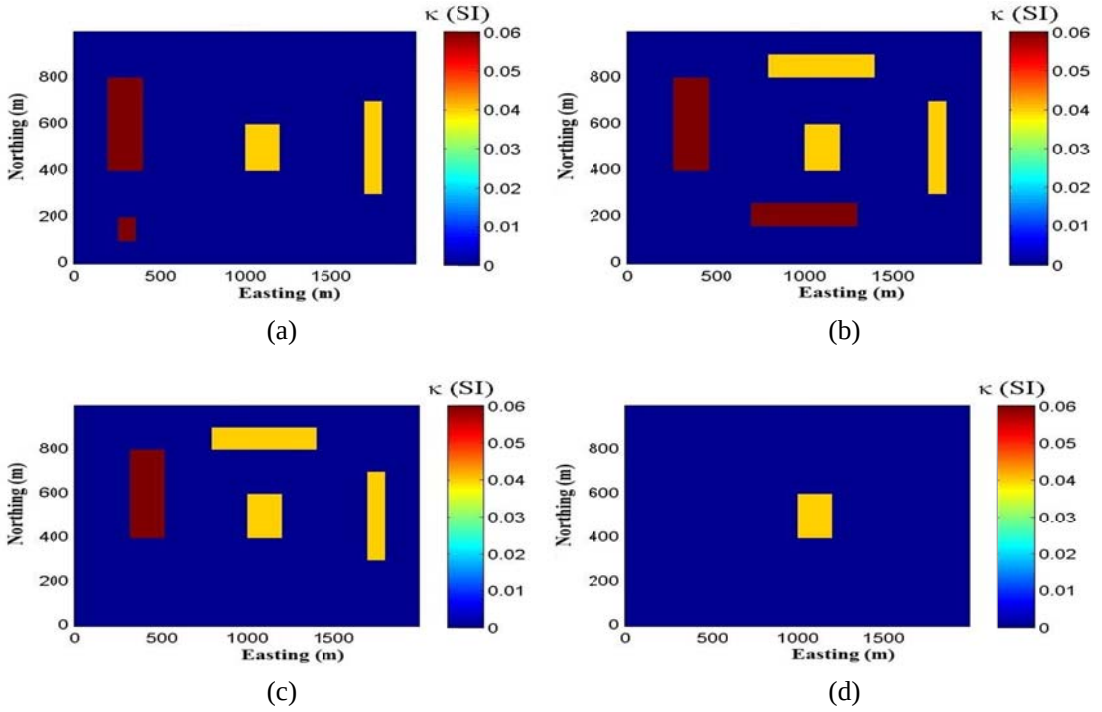

Figure 2. The model in Figure 1 is displayed in four plan-sections. The depths of the sections are: (a) 20 m; (b) 60 m; (c) 100 m; and (d) 140 m.

The inversion process is very fast, requiring less than 10 minutes to implement. The results of the algorithm for both the GCV and TGCV parameter-choice rules are given in Table 3. In each case, the final iteration (K), the final regularization parameter ($\alpha^{(K)}$), and the relative error of the reconstructed model at final iteration ($RE^{(K)}$) are reported. The results indicate that TGCV outperforms the GCV method. The plan-sections of the reconstructed model using TGCV are shown in Figure 3. The solution has horizontal borders that are in good agreement with those of the original model, but as it is typical for the inversion of magnetic data, additional structures appear at depth due to the loss of resolution. Nonetheless, unlike the smoothing inversion algorithms, the estimated model here is more focused even at depth.

Table 3. The inversion results obtained by inverting magnetic data from Figure 1b using algorithm presented in Table 1 with t=300, for TGCV and GCV as the parameter-choice methods.

Parameter-choice method	Iteration (K)	$\alpha^{(K)}$	$RE^{(K)}$
TGCV	4	190	0.8127
GCV	5	774	0.8583

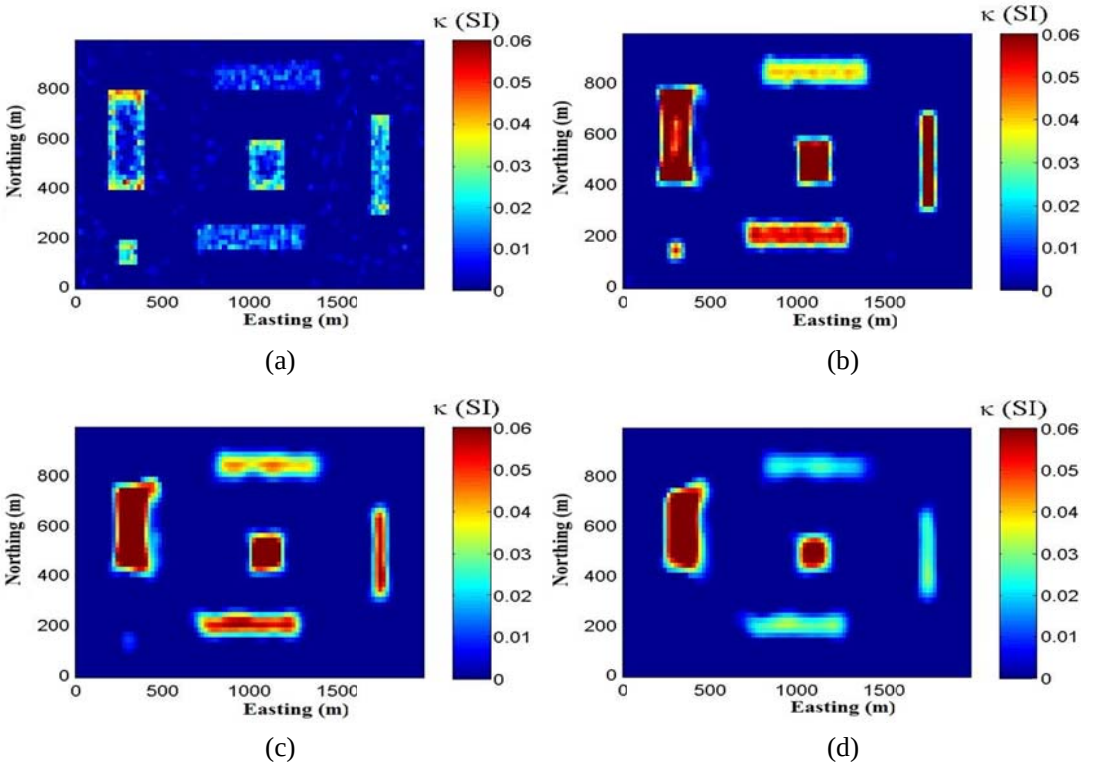

Figure 3. The reconstructed model with *t*=300 and TGCV. The depths of the sections are: (a) 20 m; (b) 60 m; (c) 100 m; and (d) 140 m.

4. Real data

The developed technique is applied for the inversion of aeromagnetic data recorded over the Wuskwatim Lake region in Manitoba, Canada (Figure 4). The given area lies within a poorly exposed meta-sedimentary gneiss belt consisting of paragneiss, amphibolite, and migmatite derived from Proterozoic volcanic and sedimentary rocks (Pilkington, 2009). Pilkington (2009) applied a data-space inversion methodology with a Cauchy norm sparsity constraint on the model parameters for the inversion of this data set, arranged in a 64×64 grid. The results of the inversion using Li and Oldenburg (1996) algorithm are also presented in Pilkington (2009). The results using the inversion algorithm presented here can therefore be compared with the inversions using both aforementioned algorithms.

Consistent with the inversion presented in Pilkington (2009), a 64×64 data grid with 100 m spacing and a uniform subsurface discretization of 64×64×20=81920 blocks are used. It is assumed that each datum is contaminated by Gaussian noise with a standard deviation of $\left(0.03\left(\boldsymbol{d}^{obs}\right)_i + 0.005\left\|\boldsymbol{d}^{obs}\right\|_2\right)$. It is emphasized that the projected problem should have a size of $t \geq m/20$, then here $t = 250$ is selected. Based on information from Pilkington (2009), the susceptibility range of $[\kappa_{\min} = 0, \kappa_{\max} = 0.2]$ is selected for the inversion. Here, the TGCV method is used for estimating the regularization parameter. The algorithm starts with $\boldsymbol{m}_{apr} = \boldsymbol{0}$ and $K_{\max} = 50$. The convergence is achieved at $K = 11$ iterations in less than 15 minutes. Two plane-sections of the recovered model at 400 m and 800 m depths are presented in Figures 5a and 5b, respectively. Furthermore, the TGCV function at final iteration is shown in Figure 5c, and an isosurface of the 3-D recovered model for susceptibilities greater than 0.05 (SI) is shown in Figure 5d. The algorithm produces results that are competitive with, but not as sparse as, those presented in Pilkington (2009, Figure 5). This is a feature of the L_1-norm algorithm applied here, as compared with sparseness constraint used in Pilkington (2009). If greater sparsity

is required, the minimum support L_0-norm stabilizer can be implemented in Table 1 by replacing W_{L1} with $W_{\mathrm{MS}} = diag\left(\left(\left(\boldsymbol{m}^{(k-1)} - \boldsymbol{m}^{(k-2)}\right)^2 + \varepsilon^2\right)^{-1/2}\right)$ in step 13 (Vatankhah et al., 2017). Furthermore, compared with the results of smoothing algorithm of Li and Oldenburg (1996), presented in Pilkington (2009, Figure 5), the results are more focused.

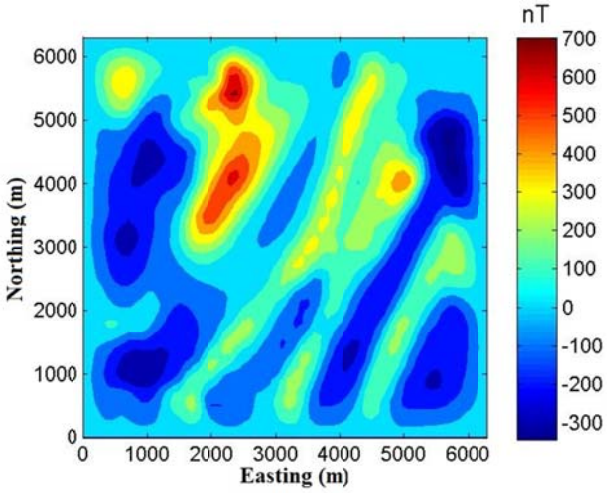

Figure 4. Aeromagnetic data over a portion of the Wuskwatin Lake area, Manitoba, Canada.

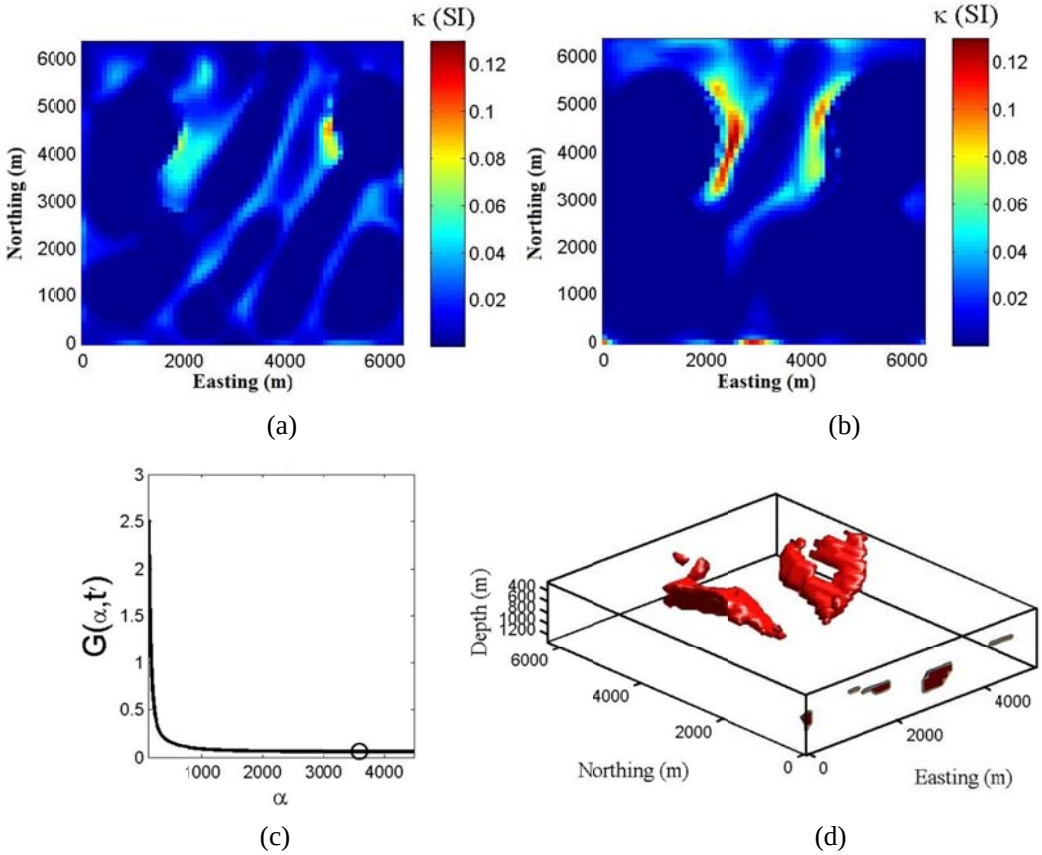

Figure 5. The results of the inversion for data in Figure 4. (a) Plane-section at depth=400 m; (b) Plane-section at depth=800 m; (c) TGCV function at final iteration and (d) The isosurface of the reconstructed model with susceptibility greater than 0.05 (SI).

5. Conclusion

An algorithm was developed for the inversion of sparse magnetic data using L_1-norm stabilization with projection of the solution to a smaller Krylov subspace using the LSQR algorithm. A truncated GCV for estimating the regularization parameter in the subspace was introduced so that the components related to the inaccurate small singular values are ignored in calculating the regularization parameter. For relatively small subspaces, acceptable solutions are obtained with a limited number of iterations for the IRLS algorithm. The algorithm was validated for a synthetic model consisting of multiple bodies, and demonstrated that the algorithm permits inversion of large data sets and produces relatively focused images of the subsurface. The results indicated that TGCV outperforms the GCV parameter-choice method. The algorithm was applied for the inversion of real aeromgnetic data collected over Wuskwatim Lake in Manitoba, Canada.

Acknowledgements

The author would like to thank Dr. Mark Pilkington for providing aeromagnetic data from Wuskwatim Lake area.

References

Boulanger, O. and Chouteau, M., 2001, Constraint in 3D gravity inversion. Geophysical prospecting, 49, 265-280.

Chung, J., Nagy, J. G. and O'Leary, D. P., 2008, A weighted GCV method for Lanczos hybrid regularization. ETNA, 28, 149-167.

Farquharson, C. G., 2008, Constructing piecewise-constant models in multidimensional minimum-structure inversions. Geophysics, 73, K1-K9.

Farquharson, C. G. and Oldenburg, D. W., 2004, A comparison of automatic techniques for estimating the regularization parameter in non-linear inverse problems. Geophys. J. Int., 156, 411-425.

Gazzola, S. and Nagy, J. G., 2014, Generalized Arnoldi_Tikhonov method for sparse reconstruction. SIAM J. Sci. Comput., 36(2), B225-B247.

Golub, G. H., Heath, M. and Wahba, G., 1979, Generalized Cross Validation as a method for choosing a good ridge parameter. Technometrics, 21(2), 215-223.

Golub, G. H. and Van Loan, C., 1996, Matrix computation, 3rd edition, John Hopkins University Press, Baltimore.

Hansen, P. C., 2007, Regularization Tools: A Matlab package for analysis and solution of discrete ill-Posed problems version 4.1 for Matlab 7.3. Numerical Algorithms, 46, 189-194.

Kilmer, M. E. and O'Leary, D. P., 2001, Choosing regularization parameters in iterative methods for ill-posed problems. SIAM Journal on Matrix Analysis and Application, 22, 1204-1221.

Last, B. J. and Kubik, K., 1983, Compact gravity inversion. Geophysics, 48, 713-721.

Li, Y. and Oldenburg, D. W., 1996, 3-D inversion of magnetic data. Geophysics, 61, 394-408.

Li, Y. and Oldenburg, D. W., 2003, Fast inversion of large-scale magnetic data using wavelet transform and a logarithmic barrier method. Geophys. J. Int., 152, 251-265.

Liu, S., Hu, X., Xi, Y., Liu, T. and Xu, S., 2015, 2D sequential inversion of total magnitude and total magnetic anomaly data affected by remanent magnetization, Geophysics, 80, K1-K12.

Loke, M. H., Acworth, I. and Dahlin, T., 2003, A comparison of smooth and blocky inversion methods in 2D electrical imaging surveys. Exploration Geophysics, 34, 182-187.

Paige, C. C. and Saunders, M. A., 1982a, LSQR: An algorithm for sparse linear equations and sparse least squares. ACM Trans. Math. Software, 8, 43-71.

Paige, C. C. and Saunders, M. A., 1982b, ALGORITHM 583 LSQR: Sparse linear equations and least squares problems. ACM Trans. Math. Software, 8, 195-209.

Pilkington, M., 1997, 3-D magnetic imaging using conjugate gradients. Geophysics, 62, 1132-1142.

Pilkington, M., 2009, 3D magnetic data-space inversion with sparseness constraint. Geophysics, 74, L7-L15.

Portniaguine, O. and Zhdanov, M. S., 1999, Focusing geophysical inversion images. Geophysics, 64, 874-887.

Portniaguine, O. and Zhdanov, M. S., 2002,

3-D magnetic inversion with data compression and image focusing. Geophysics, 67, 1532-1541.

Rao, D. B. and Babu, N. R., 1991, A rapid methods for three-dimensional modeling of magnetic anomalies. Geophysics, 56, 1729-1737.

Renaut R. A., Vatankhah, S. and Ardestani V. E., 2017, Hybrid and iteratively reweighted regularization by unbiased predictive risk and weighted GCV for projected systems. SIAM Journal on Scientific Computing, 39, 2, B221-B243.

Sun, J. and Li, Y., 2014, Adaptive L_p inversion for simultaneous recovery of both blocky and smooth features in geophysical model. Geophys. J. Int., 197, 882-899.

Vatankhah, S., Ardestani V. E. and Renaut, R. A., 2014, Automatic estimation of the regularization parameter in 2-D focusing gravity inversion: application of the method to the Safo manganese mine in northwest of Iran. Journal of Geophysics and Engineering, 11, 045001.

Vatankhah, S., Ardestani V. E. and Renaut, R. A., 2015, Application of the χ^2 principle and unbiased predictive risk estimator for determining the regularization parameter in 3D focusing gravity inversion. Geophys. J. Int., 200(1), 265-277.

Vatankhah, S., Renaut, R. A. and Ardestani, V. E., 2017, 3-D Projected L1 inversion of gravity data using truncated unbiased predictive risk estimator for regularization parameter estimation. Geophys. J. Int., 210 (3), 1872-1887.

Voronin, S., 2012, Regularization of linear systems with sparsity constraints with application to large scale inverse problems. Ph.D. thesis, Princeton University, U.S.A.

Wohlberg, B. and Rodriguez, P., 2007, An iteratively reweighted norm algorithm for minimization of total variation functionals. IEEE Signal Processing Letters, 14, 948-951.